

Phonon-induced entanglement dynamics of two donor-based charge quantum bits

F. Lastra,^{1,2} S.A. Reyes,¹ and S. Wallentowitz¹

¹*Facultad de Física, Pontificia Universidad Católica de Chile, Casilla 306, Santiago 22, Chile*

²*Departamento de Física & Center for the Development of Nanoscience and Nanotechnology, Universidad de Santiago de Chile, Casilla 307, Santiago, Chile*

(Dated: August 11, 2011)

The entanglement dynamics of a pair of donor-based charge qubits is obtained in analytical form. The disentanglement is induced by off resonant scattering of acoustical phonons in the semiconductor host. According to our results a rather unusual recovery of entanglement occurs that depends on the geometrical configuration of the qubits. In addition, for large times a non-vanishing stationary entanglement is predicted. For the cases of one and two initial excitations a simple kinetic interpretation allows for an adequate analysis of the observed dynamics. Our results also reveal a direct relation between the disentanglement rate and the inter-donor decoherence rates.

PACS numbers: 12.40.Nn, 11.55.Jy, 05.20.-y, 05.70.Fh.

I. INTRODUCTION

Quantum information processing promises highly efficient solutions to cryptographic problems and exhaustive database search, that outperform the best known algorithms with classical computers [1]. Such quantum algorithms rely on the capability to process correlations among quantum subsystems. The quantum part of these correlations is denoted as entanglement. Most commonly, the subsystems are identified as two-level systems, representing a quantum counterpart of classical bits, called quantum bits (qubits). Among the well known applications of quantum information are quantum teleportation [2], superdense coding [3], and secure distribution of cryptographic keys [4].

Entanglement, being the key ingredient of such applications, at the same time is highly fragile and can be easily deteriorated during state preparation, addressing and control of individual qubits, and final readout. Hence, it is necessary to encode quantum information in physical systems, where entanglement is protected or can be preserved in a robust way from ambient effects. Prominent examples of physical implementations are trapped ions [5], nuclear magnetic resonance [6], atoms in cavities [7], quantum dots [8], semiconductor impurities [9], superconducting qubits [10], and impurities in diamond [11].

Among the solid-state implementations [12–14] impurities embedded in a semiconductor substrate offer the advantage of comparably easy scaling and production due to highly developed fabrication techniques. The encoding of qubits in the charge degrees of freedom of pairs of donor sites allows for the addressing of individual qubits by metallic gates [15, 16]. Tunneling of the electron between donor sites together with Coulomb repulsion of electrons bound in neighboring qubits have been shown to allow for the realization of a CNOT gate [15, 17, 18]. Such a gate is the elemental building block of any quantum algorithm. Typical coherence times of such systems are limited by phonon scattering to the order of 1ps [19–21]. Therefore, the state preparation process must be faster and one may expect that entanglement is rapidly lost on this time scale.

In this work we show that to a large extent the entanglement survives beyond this time scale and therefore suffers

further degradation only from other sources of decoherence, i.e. charge fluctuations on the control electrodes. The disentanglement dynamics is obtained in analytical form showing non-Markovian features, similar to the decoherence dynamics of a single qubit [20–22]. Furthermore, it is shown that the disentanglement rate is directly related to inter-donor decoherence rates for the cases of one and two initial excitations. The structure of this rate can be explained by a simple kinetic interpretation that allows for the determination of the disentanglement rate from the geometry of the constituent donor sites.

The paper is organized as follows: In Sec. II the dynamics of a general N qubit system subject to off-resonant scattering of acoustical phonons is derived. Using these results the dynamics of entanglement between two qubits is analytically obtained in Sec. III for the cases of one and two excitations. Finally, in Sec. IV we present a summary and conclusions.

II. PHONON-INDUCED DEPHASING DYNAMICS OF QUBITS

In this chapter we deduce the dynamics of the reduced density operator of the qubit system, which is induced by off-resonant scattering of acoustical phonons within the semiconductor material. It is assumed here that $2N$ donor sites are present that conform N qubits, see Fig. 1. The results will later be specialized to the case of $N = 2$ qubits. The dynamics of a single qubit conformed by two donor sites has been derived recently by us in Ref. [20]. The present work goes beyond the case of two donors, which implies a more complex dynamics together with the possibility of studying the entanglement between pairs of qubits.

We consider the situation where a single electron is confined to each pair of donors, conforming the N qubits being centered at the positions \mathbf{r}_b , where $b = 1, \dots, N$ labels the qubit under consideration. In addition, we assume that the distances between these qubits are much larger than the inter-donor vectors \mathbf{d}_b within the qubits, i.e. $|\mathbf{r}_b - \mathbf{r}_{b'}| \gg |\mathbf{d}_{b'}|$. Under these circumstances the tunneling of electrons between different qubits can be safely neglected. Considering the in-

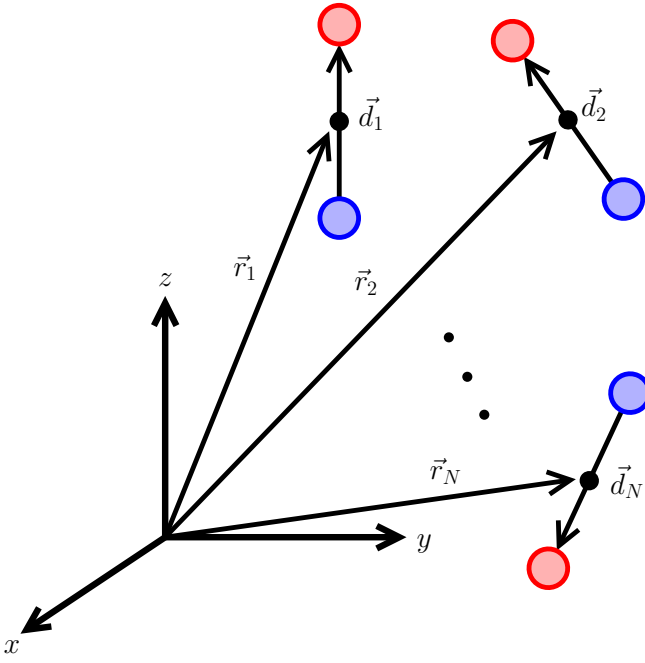


Figure 1: Geometrical setup of N qubits formed by $2N$ donor sites in a semiconductor material. Blue and red donor sites correspond to qubit states $m_b = -\frac{1}{2}$ and $m_b = +\frac{1}{2}$, respectively, where $b = 1, \dots, N$ denotes the qubit. Each qubit b has an inter-site distance \mathbf{d}_b pointing from site $m_b = -\frac{1}{2}$ to $m_b = +\frac{1}{2}$, and a position vector \mathbf{r}_b pointing towards the center of the qubit.

teraction of the qubit charges with acoustical phonons in the semiconductor substrate at room temperature or below, off-resonant phonon scattering is the main source of decoherence in the electron dynamics [20]. This type of electron-phonon interaction is accurately described by the spin-boson Hamiltonian

$$\hat{H} = \hbar \sum_b (\omega_b \hat{S}_{b,z} + \Delta_b \hat{S}_{b,x}) + \sum_{\mathbf{k}} \hbar \omega_{\mathbf{k}} \hat{a}_{\mathbf{k}}^\dagger \hat{a}_{\mathbf{k}} + \hbar \sum_b \hat{S}_{b,z} \sum_{\mathbf{k}} (g_{b,\mathbf{k}} \hat{a}_{\mathbf{k}}^\dagger + g_{b,\mathbf{k}}^* \hat{a}_{\mathbf{k}}), \quad (1)$$

where the individual interaction rate of the m_b th donor site ($m_b = \pm 1/2$) within qubit b reads

$$g_{b,\mathbf{k}} = \frac{D}{\hbar s} \sqrt{\frac{2\hbar \omega_{\mathbf{k}}}{M_0}} \sum_{m_b = \pm 1/2} \frac{m_b e^{-i\mathbf{k} \cdot (\mathbf{r}_b + m_b \mathbf{d}_b)}}{\left[1 + \left(\frac{ka_{b,m_b}}{2}\right)^2\right]^2}. \quad (2)$$

Here $\hat{a}_{\mathbf{k}}$ are the annihilation operators of longitudinal acoustical phonon with dispersion relation $\omega_{\mathbf{k}} = sk$, s being the sound speed. Moreover, M_0 and D are the mass within a unit cell of the semiconductor and the deformation constant, respectively. Each donor site is described by a s -wave ground-state with Bohr radius a_{b,m_b} and the electronic transition of each qubit b

is generated by the pseudo spin- $\frac{1}{2}$ operator \hat{S}_b , where

$$\hat{S}_{b,z} = \frac{1}{2} \left(\left| \mathbf{r}_b + \frac{\mathbf{d}_b}{2} \right\rangle \left\langle \mathbf{r}_b + \frac{\mathbf{d}_b}{2} \right| - \left| \mathbf{r}_b - \frac{\mathbf{d}_b}{2} \right\rangle \left\langle \mathbf{r}_b - \frac{\mathbf{d}_b}{2} \right| \right), \quad (3)$$

with $|\mathbf{r}_b \pm \mathbf{d}_b/2\rangle$ being the states with the electron being localized at the corresponding donor site. In what follows we assume that during the free evolution of the system, tunneling is inhibited by either an applied potential barrier between the donor sites, or due to a strong bias between the qubit levels, $|\omega_b| \gg |\Delta_b|$, which can be provided for by the application of a DC electric field.

Following the same steps as in Ref. [20], the Hamiltonian Eq.(1) can be diagonalized, to obtain the complete set of eigenstates as displaced number states

$$|E_{\{m_b\}, \{N_{\mathbf{k}}\}}\rangle = |\{m_b\}\rangle \otimes \hat{D}^\dagger(\{\alpha_{\{m_b\}, \mathbf{k}}\}) |\{N_{\mathbf{k}}\}\rangle, \quad (4)$$

with eigenenergies

$$E_{\{m_b\}, \{N_{\mathbf{k}}\}} = \hbar \sum_b \omega_b m_b + \sum_{\mathbf{k}} \hbar \omega_{\mathbf{k}} N_{\mathbf{k}}. \quad (5)$$

Here the multi-mode displacement operator reads

$$\hat{D}(\{\alpha_{\mathbf{k}}\}) = \exp \left[\sum_{\mathbf{k}} (\alpha_{\mathbf{k}} \hat{a}_{\mathbf{k}}^\dagger - \alpha_{\mathbf{k}}^* \hat{a}_{\mathbf{k}}) \right], \quad (6)$$

and $|\{N_{\mathbf{k}}\}\rangle = \prod_{\mathbf{k}} |N_{\mathbf{k}}\rangle$ are multi-mode number states of the acoustic phonons and the displacement amplitude reads

$$\alpha_{\{m_b\}, \mathbf{k}} = \sum_b m_b \alpha_{b,\mathbf{k}}, \quad (7)$$

where $\alpha_{b,\mathbf{k}} = g_{b,\mathbf{k}}/\omega_{\mathbf{k}}$. Furthermore, the quantum state of the qubits is encoded in the register state

$$|\{m_b\}\rangle = |m_1\rangle \otimes |m_2\rangle \otimes \dots \otimes |m_N\rangle, \quad (8)$$

where each of the qubits can be in states $|m_b = \pm \frac{1}{2}\rangle$ ($b = 1, \dots, N$).

Given the eigenstates (4) and eigenenergies (5), the general solution of the reduced density operator of the qubits, i.e. traced over the phonons, reads

$$\hat{\rho}(t) = \sum_{\{m_b\}, \{s_b\}} |\{m_b\}\rangle \langle \{s_b\}| \sum_{\{N_{\mathbf{k}}\}} \sum_{\{N'_{\mathbf{k}}\}} \rho_{\{m_b\}, \{N_{\mathbf{k}}\}; \{s_b\}, \{N'_{\mathbf{k}}\}} \times \langle \{N'_{\mathbf{k}}\} | \hat{D}(\{\alpha_{\{s_b\}, \mathbf{k}}\}) \hat{D}^\dagger(\{\alpha_{\{m_b\}, \mathbf{k}}\}) |\{N_{\mathbf{k}}\}\rangle \times \exp \left[-\frac{it}{\hbar} (E_{\{m_b\}, \{N_{\mathbf{k}}\}} - E_{\{s_b\}, \{N'_{\mathbf{k}}\}}) \right]. \quad (9)$$

Here the matrix elements of the initial density operator of the complete electron-phonon system in the basis of the energy eigenstates (4) are

$$\rho_{\{m_b\}, \{N_{\mathbf{k}}\}; \{s_b\}, \{N'_{\mathbf{k}}\}} = \langle E_{\{m_b\}, \{N_{\mathbf{k}}\}} | \hat{\rho}(0) | E_{\{s_b\}, \{N'_{\mathbf{k}}\}} \rangle. \quad (10)$$

These density matrix elements are determined by the state-preparation process that is utilized to set up the initial entanglement between the qubits. A generic state-preparation process can be described as follows:

We assume that initially the system is at low enough temperature, $k_B T \ll \hbar \omega_b$, such that it has relaxed completely into a state where all the qubits are in their lowest energy states, $m_b = -1/2$ ($b = 1, \dots, N$), and coexist in thermal equilibrium with the phonons in the substrate. Starting from this state the system undergoes a state preparation process in which the qubits can be coherently transferred into a superposition of ground and excited states, without affecting the quantum state of the phonons. The probability amplitudes to transfer from the initial qubit state $\{-\frac{1}{2}, -\frac{1}{2}, \dots, -\frac{1}{2}\}$ to the qubit states $\{m_b\}$, shall be denoted by $\Psi_{\{m_b\}}$. The corresponding transition can be generated by the application of the operator

$$\hat{S}_{+, \{m_b\}} = \Pi_b \left[\delta_{m_b, \frac{1}{2}} \hat{S}_{+, b} + \left(1 - \delta_{m_b, \frac{1}{2}}\right) \hat{I}_b \right], \quad (11)$$

where \hat{I}_b is the identity operator in the Hilbert space of qubit b . Thus, the matrix elements of the prepared initial state (10) become

$$\rho_{\{m_b\}, \{N_{\mathbf{k}}\}; \{s_b\}, \{N'_{\mathbf{k}}\}} = \Psi_{\{m_b\}} \Psi_{\{s_b\}}^* \langle E_{\{m_b\}, \{N_{\mathbf{k}}\}} | \hat{S}_{+, \{m_b\}} \hat{\rho}_T \hat{S}_{+, \{s_b\}}^\dagger | E_{\{s_b\}, \{N'_{\mathbf{k}}\}} \rangle, \quad (12)$$

where

$$\hat{\rho}_T = \sum_{\{N_{\mathbf{k}}\}} P_{\{N_{\mathbf{k}}\}} | E_{\{-1/2, -1/2, \dots, -1/2\}, \{N_{\mathbf{k}}\}} \rangle \langle E_{\{-1/2, -1/2, \dots, -1/2\}, \{N_{\mathbf{k}}\}} | \quad (13)$$

is the initial thermal state with the phonon statistics

$$P_{\{N_{\mathbf{k}}\}} = Z^{-1} \exp \left(- \sum_{\mathbf{k}} \beta_k N_{\mathbf{k}} \right), \quad (14)$$

with Z satisfying $\sum_{\{N_{\mathbf{k}}\}} P_{\{N_{\mathbf{k}}\}} = 1$, and $\beta_k = \hbar \omega_k / (k_B T)$.

We note that the corresponding prepared initial reduced density operator of the qubits is pure, i.e. is of the form $|\psi(0)\rangle \langle \psi(0)|$ with the qubit state being the sought superposition

$$|\psi(0)\rangle = \sum_{\{m_b\}} \Psi_{\{m_b\}} |\{m_b\}\rangle. \quad (15)$$

Thus, the presence of the phonons does not prevent a coherent preparation of the initial qubit state. However, the initial state preparation takes the electron-phonon system out of thermal equilibrium so that the decoherence of the quantum state of the qubits cannot be treated by the usual method of spectral functions [23].

The generic state preparation, as described above, can be implemented for example by switching the gate voltages so that the on-site energies within a qubit cross each other inducing Landau-Zener transitions. At the end of the process, the system will be in a coherent superposition of all possible

states of the system depending on how fast its two-level components were driven across the level crossing. Alternatively, it may be implemented by time controlled tunneling and employing the Coulomb repulsion between neighboring qubits to generate entangled qubit states, as proposed for implementing CNOT gates [15, 17, 18]. Furthermore, it could also be implemented by THz Raman transitions between the donor sites [24].

We note that the matrix elements of the initial *reduced* electronic density operator are obtained from Eq. (9) as

$$\langle \{m_b\} | \hat{\rho}_S(0) | \{s_b\} \rangle = \sum_{\{N_{\mathbf{k}}\}} \sum_{\{N'_{\mathbf{k}}\}} \rho_{\{m_b\}, \{N_{\mathbf{k}}\}; \{s_b\}, \{N'_{\mathbf{k}}\}} \times f_{\{s_b\}, \{N'_{\mathbf{k}}\}; \{m_b\}, \{N_{\mathbf{k}}\}}, \quad (16)$$

with the non-diagonal elements containing the Franck–Condon type transition amplitudes

$$f_{\{s_b\}, \{N'_{\mathbf{k}}\}; \{m_b\}, \{N_{\mathbf{k}}\}} = \langle \{N'_{\mathbf{k}}\} | \hat{D}(\{\alpha_{\{s_b\}, \mathbf{k}}\}) \hat{D}^\dagger(\{\alpha_{\{m_b\}, \mathbf{k}}\}) | \{N_{\mathbf{k}}\} \rangle. \quad (17)$$

These factors are overlap integrals of two displaced phonon number states with displacements $\alpha_{\{s_b\}, \mathbf{k}}$ and $\alpha_{\{m_b\}, \mathbf{k}}$, respectively. Their presence is due to the fact that the initial density matrix of the complete electron-phonon system (10) is in the basis of the energy eigenstates (4), whereas the matrix elements of Eq. (16) are in the basis of the product states $|\{m_b\}\rangle \otimes |\{N_{\mathbf{k}}\}\rangle$ that differ by the displacement of the phonons.

Consistent with a dephasing model, the diagonal elements follow from Eq. (9) as invariants:

$$\langle \{m_b\} | \hat{\rho}_S(t) | \{m_b\} \rangle = \langle \{m_b\} | \hat{\rho}_S(0) | \{m_b\} \rangle. \quad (18)$$

However, this dephasing — being induced by off-resonant scattering of acoustical phonons — modifies the time evolution of the off-diagonal density matrix elements as

$$\begin{aligned} \langle \{m_b\} | \hat{\rho}_S(t) | \{s_b\} \rangle &= e^{-i \sum_b (m_b - s_b) \omega_b t} \\ &\times \sum_{\{N_{\mathbf{k}}\}} \sum_{\{N'_{\mathbf{k}}\}} \rho_{\{m_b\}, \{N_{\mathbf{k}}\}; \{s_b\}, \{N'_{\mathbf{k}}\}} \\ &\times f_{\{s_b\}, \{N'_{\mathbf{k}}\}; \{m_b\}, \{N_{\mathbf{k}}\}} e^{-i \sum_{\mathbf{k}} \omega_k (N_{\mathbf{k}} - N'_{\mathbf{k}}) t}. \end{aligned} \quad (19)$$

It can be observed in Eq. (19) that apart from the free oscillation with angular frequency ω_0 , a dephasing is induced by differing phonon numbers in combination with the presence of the Franck–Condon factor.

To further evaluate the dephasing of the off-diagonal density matrix elements of the N qubits, we insert the initial complete density matrix elements (10) together with Eq. (13) into Eq. (19). From this we obtain

$$\langle \{m_b\} | \hat{\rho}_S(t) | \{s_b\} \rangle = \Psi_{\{m_b\}} \Psi_{\{s_b\}}^* e^{-i \sum_b (m_b - s_b) \omega_b t} \sum_{\{M_{\mathbf{k}}\}} P_{\{M_{\mathbf{k}}\}} \sum_{\{N_{\mathbf{k}}\}} \sum_{\{N'_{\mathbf{k}}\}} e^{-i \sum_{\mathbf{k}} \omega_k (N_{\mathbf{k}} - N'_{\mathbf{k}}) t}$$

$$\times \times f_{\{s_b\},\{N'_k\};\{-\frac{1}{2},\dots,-\frac{1}{2}\},\{M_k\}}^* f_{\{s_b\},\{N'_k\};\{m_b\},\{N_k\}} f_{\{m_b\},\{N_k\};\{-\frac{1}{2},\dots,-\frac{1}{2}\},\{M_k\}}. \quad (20)$$

Employing the thermal phonon statistics (14) the sum over the phonon numbers in Eq. (20) can be rewritten as a trace, which leaves us with

$$\begin{aligned} \langle \{m_b\} | \hat{\rho}_S(t) | \{s_b\} \rangle &= \Psi_{\{m_b\}} \Psi_{\{s_b\}}^* e^{-i\sum_b(m_b-s_b)\omega_b t} Z^{-1} \text{Tr} \left[\hat{D}(\{\alpha_{\{-\frac{1}{2},\dots,-\frac{1}{2}\},\mathbf{k}\}}) \hat{D}^\dagger(\{\alpha_{\{s_b\},\mathbf{k}\}}) \right. \\ &\times \hat{D}(\{\alpha_{\{s_b\},\mathbf{k}\}}) \hat{D}^\dagger(\{\alpha_{\{m_b\},\mathbf{k}\}}) \hat{D}(\{\alpha_{\{m_b\},\mathbf{k}\}}) \hat{D}^\dagger(\{\alpha_{\{-\frac{1}{2},\dots,-\frac{1}{2}\},\mathbf{k}\}}) e^{-\sum_k \beta_k \hat{N}_k} \left. \right], \quad (21) \end{aligned}$$

where we defined the time-dependent phonon displacement amplitude $\alpha_{\{m_b\},\mathbf{k}}(t) = \alpha_{\{m_b\},\mathbf{k}} \exp(-i\omega_k t)$. The displacement operators in Eq. (21) can be combined to obtain

$$\begin{aligned} \langle \{m_b\} | \hat{\rho}_S(t) | \{s_b\} \rangle &= \Psi_{\{m_b\}} \Psi_{\{s_b\}}^* e^{-i\sum_b(m_b-s_b)\omega_b t + i\Delta_{\{m_b\},\{s_b\}}(t)} \\ &\times Z^{-1} \text{Tr} \left[\hat{D}(\delta_{\{m_b\},\{s_b\},\mathbf{k}}(1 - e^{-i\omega_k t})) e^{-\sum_k \beta_k \hat{N}_k} \right], \quad (22) \end{aligned}$$

with the time dependent phase being

$$\Delta_{\{m_b\},\{s_b\}}(t) = \Im \sum_{\mathbf{k}} \bar{\alpha}_{\{m_b\},\{s_b\},\mathbf{k}} \delta_{\{m_b\},\{s_b\},\mathbf{k}}^* (e^{i\omega_k t} - 1) \quad (23)$$

Here we have defined sum and difference displacements:

$$\bar{\alpha}_{\{m_b\},\{s_b\},\mathbf{k}} = \alpha_{\{m_b\},\mathbf{k}} + \alpha_{\{s_b\},\mathbf{k}} - 2\alpha_{\{-\frac{1}{2},\dots,-\frac{1}{2}\},\mathbf{k}}, \quad (24)$$

$$\delta_{\{m_b\},\{s_b\},\mathbf{k}} = \alpha_{\{m_b\},\mathbf{k}} - \alpha_{\{s_b\},\mathbf{k}}. \quad (25)$$

The trace in Eq. (22) represents a thermal average that can be evaluated in phase space to obtain

$$\begin{aligned} \langle \{m_b\} | \hat{\rho}_S(t) | \{s_b\} \rangle &= \Psi_{\{m_b\}} \Psi_{\{s_b\}}^* e^{-i\sum_b(m_b-s_b)\omega_b t + i\Delta_{\{m_b\},\{s_b\}}(t)} \\ &\times \exp \left\{ - \int_0^t dt' \Gamma_{\{m_b\},\{s_b\}}(t') \right\}, \quad (26) \end{aligned}$$

where the decoherence rate of the qubit state is defined as

$$\Gamma_{\{m_b\},\{s_b\}}(t) = \sum_{b,b'} (m_b - s_b)(m_{b'} - s_{b'}) \gamma_{b,b'}(t). \quad (27)$$

Whereas this rate depends on the quantum numbers of the density matrix element under consideration, the relation of pairs of bits is governed by the inter-bit decorrelation rate, given by

$$\gamma_{b,b'}(t) = 4 \sum_{m_b} \sum_{s_{b'}} m_b s_{b'} \gamma(t; a_{b,m_b}, a_{b',s_{b'}}, l_{b,m_b;b',s_{b'}}). \quad (28)$$

This rate in turn depends via the inter-donor decoherence rate $\gamma(t; a, a', l)$ on the Bohr radii of the four donor sites of the two qubits and on the six possible distances between these four donors,

$$l_{b,m_b;b',s_{b'}} = |(\mathbf{r}_b + m_b \mathbf{d}_b) - (\mathbf{r}_{b'} + s_{b'} \mathbf{d}_{b'})|. \quad (29)$$

Moreover, the inter-donor decoherence rate is obtained from Eqs. (22) – (29) as

$$\gamma(t; a, a', l) = \Gamma_T \left[\left(\frac{aa_B}{a^2 - a'^2} \right)^2 \sum_{\sigma=\pm 1} \sigma \left(\frac{|l - \sigma st|}{l} + \frac{a}{2l} \frac{a^2 - 5a'^2}{a^2 - a'^2} \right) e^{-2|l - \sigma st|/a} + (a \leftrightarrow a') \right]. \quad (30)$$

In this expression the temperature dependent rate reads $\Gamma_T = \omega_B(T/T_B)$, where the convenient temperature scale is chosen as

$$k_B T_B = N_B M_0 s^2 \left(\frac{\hbar \omega_B}{D} \right)^2. \quad (31)$$

Here $\omega_B = 2\pi s/a_B$ with a_B being the average Bohr radius of

all donor sites and N_B is the number of unit cells within the average Bohr volume a_B^3 .

In the limit of identical donor sites, $a_{b,m_b} \rightarrow a_B$ ($b = 1, \dots, N$), the inter-donor decoherence rate (30) approaches the form $\gamma(t; a, a', l) \rightarrow \gamma(t; l)$ with

$$\gamma(t; l) = \Gamma_T \frac{a_B}{l} \sum_{\sigma=\pm 1} \sigma \left[\frac{1}{6} \left(\frac{|l - \sigma st|}{a_B} \right)^3 + \frac{1}{2} \left(\frac{|l - \sigma st|}{a_B} \right)^2 + \frac{5}{8} \left(\frac{|l - \sigma st|}{a_B} \right) + \frac{5}{16} \right] e^{-2|l - \sigma st|/a_B}. \quad (32)$$

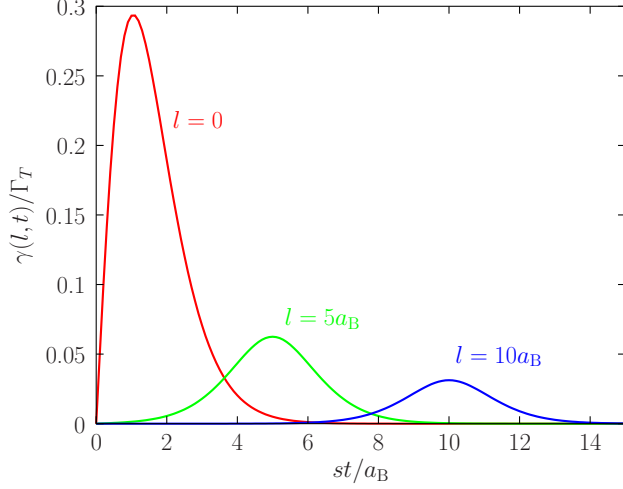


Figure 2: Dimensionless and temperature independent inter-site decoherence rate $\gamma(l, t)/\Gamma_T$ as a function of the traveled distance of a phonon in units of the Bohr radius, st/a_B .

We note that in the limit of vanishing distance between donor sites, $l \rightarrow 0$, this function becomes

$$\gamma(t; 0) = \Gamma_T \left[\frac{2}{3} \left(\frac{st}{a_B} \right)^3 + \left(\frac{st}{a_B} \right)^2 + \frac{1}{2} \left(\frac{st}{a_B} \right) \right] e^{-2st/a_B}. \quad (33)$$

This is a function peaked at $t \sim a_B/s$, i.e. at the time a phonon needs to travel the distance of one Bohr radius, see Fig. 2 (red curve). Different from this special case ($l \rightarrow 0$) for $l > 0$ the inter-donor decoherence rate is peaked at the time $t \sim l/s$ that is required for a phonon to travel the distance l , see Fig. 2 (green and blue curves).

III. DYNAMICS OF ENTANGLEMENT BETWEEN TWO QUBITS

In the following we will discuss the special case of two qubits being present in the semiconductor system, i.e. $N = 2$. In this case the state of the qubits $|\{m_b\}\rangle$ with $b = 1, 2$ lives in a four-dimensional Hilbert space and the entanglement of this bipartite system can be described by the concurrence C [25]. This quantity is a measure of entanglement bounded in the range between zero and one, with the maximum entanglement corresponding to unit concurrence. On the other hand, for separable states, lacking any entanglement, the concurrence is zero.

Furthermore, due to the pure dephasing effect of the phonon scattering, no transitions of the qubits are induced. Therefore, the phonon scattering will transform an initial general superposition state

$$|\psi(0)\rangle = \sum_{m_1, m_2 = \pm \frac{1}{2}} \Psi_{\{m_1, m_2\}} |\{m_1, m_2\}\rangle, \quad (34)$$

into a non-pure statistical mixture of only those states that initially already existed. Thus, during the time evolution the den-

sity operator stays within the Hilbert sub space defined by the initial state. This feature allows us to separately treat the two prominent cases of having initially one or two ‘‘excitations’’, respectively.

A. Case of one excitation

Assume the initial state of the two qubits to be of the form

$$|\psi(0)\rangle = \Psi_{\{\frac{1}{2}, -\frac{1}{2}\}} |\{\frac{1}{2}, -\frac{1}{2}\}\rangle + \Psi_{\{-\frac{1}{2}, \frac{1}{2}\}} |\{-\frac{1}{2}, \frac{1}{2}\}\rangle. \quad (35)$$

Since only one of the qubits is in its ‘‘excited’’ state, this superposition is usually denoted as the ‘‘one excitation’’ case. Choosing the basis vectors of the bipartite system as $\{|\{\frac{1}{2}, \frac{1}{2}\}\rangle, |\{\frac{1}{2}, -\frac{1}{2}\}\rangle, |{-\frac{1}{2}, \frac{1}{2}\}\rangle, |{-\frac{1}{2}, -\frac{1}{2}\}\rangle\}$, following Eq. (26) the time-dependent density matrix can be written as

$$\rho_S(t) = \begin{pmatrix} 0 & 0 & 0 & 0 \\ 0 & \rho_{\{\frac{1}{2}, -\frac{1}{2}\}, \{\frac{1}{2}, -\frac{1}{2}\}}(t) & \rho_{\{\frac{1}{2}, -\frac{1}{2}\}, \{-\frac{1}{2}, \frac{1}{2}\}}(t) & 0 \\ 0 & \rho_{\{\frac{1}{2}, -\frac{1}{2}\}, \{-\frac{1}{2}, \frac{1}{2}\}}^*(t) & \rho_{\{-\frac{1}{2}, \frac{1}{2}\}, \{-\frac{1}{2}, \frac{1}{2}\}}(t) & 0 \\ 0 & 0 & 0 & 0 \end{pmatrix}. \quad (36)$$

For this particular form of the density matrix, the concurrence simplifies to

$$C(t) = 2 \left| \rho_{\{\frac{1}{2}, -\frac{1}{2}\}, \{-\frac{1}{2}, \frac{1}{2}\}}(t) \right|. \quad (37)$$

Inserting the corresponding density matrix element from Eq. (26) into Eq. (37), the concurrence results as

$$C(t) = 2\sqrt{p(1-p)} \exp \left[- \int_0^t dt' \Gamma_{\{\frac{1}{2}, -\frac{1}{2}\}, \{-\frac{1}{2}, \frac{1}{2}\}}(t') \right], \quad (38)$$

where $p = |\Psi_{\{\frac{1}{2}, -\frac{1}{2}\}}|^2$ is the initial probability for the two qubits being in state $|\{\frac{1}{2}, -\frac{1}{2}\}\rangle$. The maximum initial concurrence is of course obtained for equal weights, $p = 1/2$, of the two constituent states.

From Eq. (38) it becomes apparent that the decoherence rate of the state of the qubits acts as disentanglement rate. This rate is shown in Fig. 3 for qubits with $d = 10a_B$, an inter-qubit distance of $20a_B$, and a relative angle of 45° , see inset of Fig. 3. It shows a series of alternating maxima and minima at increasing times. The principal positive maximum at the beginning occurs at $t \approx a_B/s$, which is the time needed by the phonon to travel within a donor site. This is the main source of disentanglement. The times of the subsequent extrema can be identified as the travel times between pairs of donor sites, as indicated in the inset of Fig. 3. Whereas the positive maxima destroy, the negative minima restore the entanglement between the qubits. The mapping of which phonon path between donor sites leads to positive or negative extrema in the disentanglement rate can be established as follows:

The concurrence is given by the modulus of the density matrix element $\rho_{\{\frac{1}{2}, -\frac{1}{2}\}, \{-\frac{1}{2}, \frac{1}{2}\}}(t)$ that describes the time-dependent correlation between states $|\{-\frac{1}{2}, \frac{1}{2}\}\rangle$ and $|\{\frac{1}{2}, -\frac{1}{2}\}\rangle$. Correlations between these states can only be created when a phonon travels between a donor site occupied by

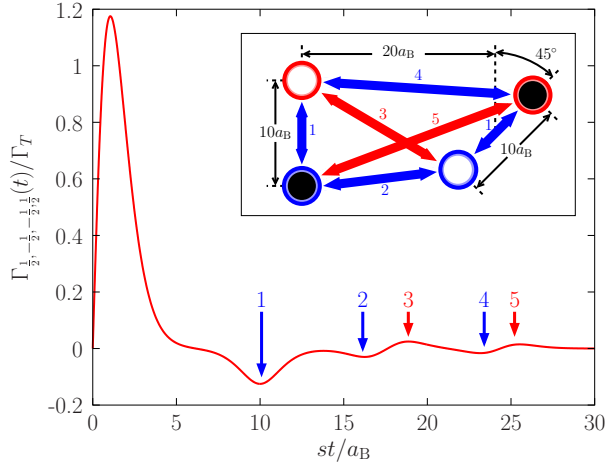


Figure 3: Dimensionless disentanglement rate $\Gamma_{\{\frac{1}{2}, -\frac{1}{2}\}\{-\frac{1}{2}, \frac{1}{2}\}}(t)/\Gamma_T$ as a function of the dimensionless time st/a_B for the case of a single excitation. The inset shows the geometrical configuration of the donor sites: $d_1 = d_2 = 10a_B$, $|\mathbf{r}_1 - \mathbf{r}_2| = 20a_B$, 45° angle between qubit axes. The rounded lengths of the inter-donor distances in units of a_B are: $l/a_B = 10$ (1), 16.53 (2), 18.6 (3), 23.6 (4), 25.0 (5).

one state to another donor site that is occupied by the other state. The corresponding site occupations of each of the states involved are indicated in the inset of Fig. 3 by black and white colors, respectively. The sites of each qubit are marked by blue for $m_b = -\frac{1}{2}$ and red for $m_b = +\frac{1}{2}$. With this color scheme, the creation of correlations mediated by sound waves is produced via phonon travels between a black and a white donor site.

These phonon travels are: the passage within the individual qubits for the distance $10a_B$, that produces in Fig. 3 the negative minimum 1, and the passages between blue and red sites at distances $\approx 16.5a_B$ and $\approx 23.6a_B$, that produce the minima 2 and 4. All the other phonon passages produce decorrelation and destroy the entanglement at distances $\approx 18.6a_B$ and $\approx 25.0a_B$, which generate the positive maxima 3 and 5 in Fig. 3.

We note that diminishing the 45° angle between the qubit axes results in lengths 2 and 4, and lengths 3 and 5, respectively, becoming progressively comparable. In the limiting case of two collinear qubits, i.e. 0° angle, these pairs of lengths are identical so that as a consequence the disentanglement rate shows only two positive and two negative peaks, as shown in Fig. 4 (a). On the other hand, as one approaches the limiting angle of 90° , i.e. the CNOT configuration [15, 17, 18], the extrema first sparse and finally peaks 2 and 4 cancel peaks 3 and 5, respectively. As a result, the disentanglement rate shows only the principal positive peak at $t \approx a_B/s$, see Fig. 4 (b).

The evolution of the concurrence for the case of 45° between qubit axes is shown in Fig. 5. It can be seen that a stationary and non-vanishing value of the concurrence is reached for large times. Moreover, the temperature dependence indicates an only minor loss of entanglement at temperatures $T/T_B < 0.01$. Given that for P impurities embedded in

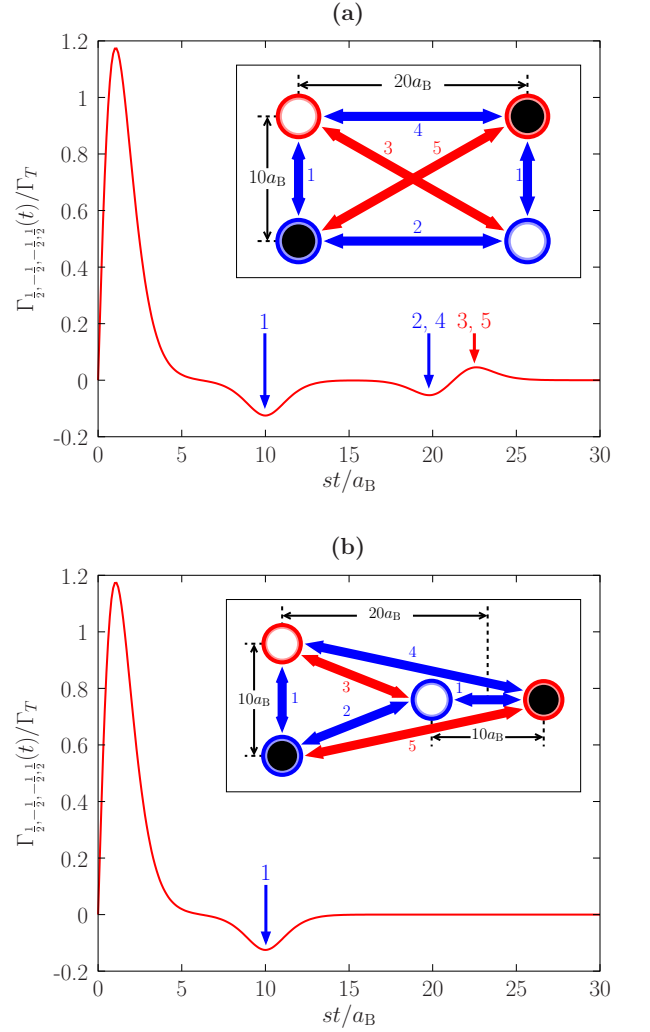


Figure 4: Dimensionless disentanglement rate $\Gamma_{\{\frac{1}{2}, -\frac{1}{2}\}\{-\frac{1}{2}, \frac{1}{2}\}}(t)/\Gamma_T$ as a function of the dimensionless time st/a_B for the case of a single excitation. Same parameters as in Fig. 3, but for collinear (a) and perpendicular (b) qubits.

a Si substrate the characteristic temperature is of the order of $T_B \sim 300\text{K}$, this case corresponds to liquid He temperatures.

B. Case of two excitations

The other prominent case is that of initial two excitations. This case is described by the initial state being of the form

$$|\psi(0)\rangle = \psi_{\{\frac{1}{2}, \frac{1}{2}\}}|\{\frac{1}{2}, \frac{1}{2}\}\rangle + \psi_{\{-\frac{1}{2}, -\frac{1}{2}\}}|\{-\frac{1}{2}, -\frac{1}{2}\}\rangle. \quad (39)$$

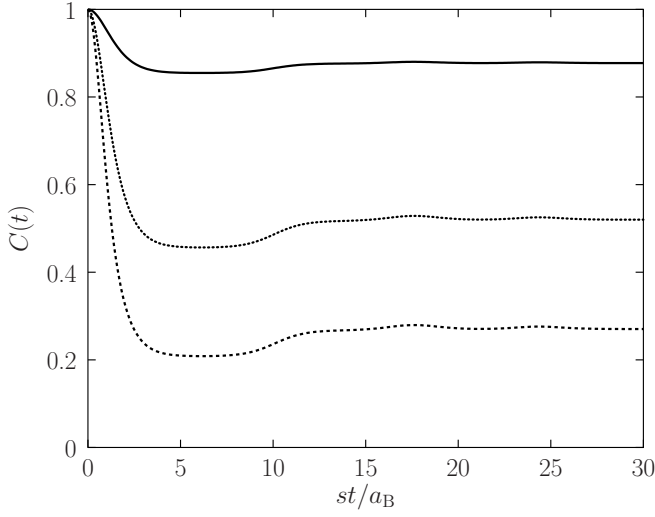


Figure 5: Concurrence as a function of the dimensionless time st/a_B for the case of a single excitation for temperatures $T/T_B = 0.01$ (solid curve), 0.05 (dotted curve), 0.1 (dashed curve). Other parameters same as in Fig. 3 with $p = 1/2$.

In the same standard basis as before, the time-dependent density matrix results then as

$$\rho(t) = \begin{pmatrix} \rho_{\{\frac{1}{2}, \frac{1}{2}\}, \{\frac{1}{2}, \frac{1}{2}\}}(t) & 0 & 0 & \rho_{\{\frac{1}{2}, \frac{1}{2}\}, \{-\frac{1}{2}, -\frac{1}{2}\}}(t) \\ 0 & 0 & 0 & 0 \\ 0 & 0 & 0 & 0 \\ \rho_{\{\frac{1}{2}, \frac{1}{2}\}, \{-\frac{1}{2}, -\frac{1}{2}\}}^*(t) & 0 & 0 & \rho_{\{-\frac{1}{2}, -\frac{1}{2}\}, \{-\frac{1}{2}, -\frac{1}{2}\}}(t) \end{pmatrix}. \quad (40)$$

Also for this case the concurrence simplifies to a simple expression, given by

$$C(t) = 2 \left| \rho_{\{\frac{1}{2}, \frac{1}{2}\}, \{-\frac{1}{2}, -\frac{1}{2}\}}(t) \right|, \quad (41)$$

which, after insertion of Eq. (40), becomes

$$C(t) = 2\sqrt{p(1-p)} \exp \left[- \int_0^t dt' \Gamma_{\{\frac{1}{2}, \frac{1}{2}\}, \{-\frac{1}{2}, -\frac{1}{2}\}}(t') \right], \quad (42)$$

where now $p = |\psi_{\{\frac{1}{2}, \frac{1}{2}\}}|^2$ is the probability for the two qubits being “excited”. From the change of indices it can be easily seen that, apart from the first positive and first negative peak, the signs of the peaks of the disentanglement rate are reversed as compared to the corresponding one excitation case, see Fig. 6.

IV. SUMMARY AND OUTLOOK

In this paper we considered the time evolution of entanglement in donor-based charge qubits that is induced by off-

resonant scattering with acoustical phonons. We showed that this system can be solved analytically and that a non-Markovian behavior emerges with negative disentanglement rates, leading to non-monotonic disentanglement in time.

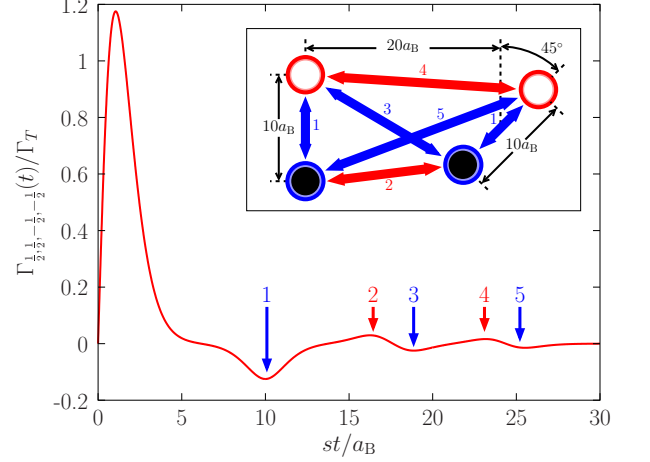


Figure 6: Dimensionless disentanglement rate $\Gamma_{\{\frac{1}{2}, \frac{1}{2}\}, \{-\frac{1}{2}, -\frac{1}{2}\}}(t)/\Gamma_T$ as a function of the dimensionless time st/a_B for the case of two excitations. The inset shows the geometrical configuration of the donor sites: $d_1 = d_2 = 10a_B$, $|\mathbf{r}_1 - \mathbf{r}_2| = 20a_B$, 45° angle between qubit axes. The rounded lengths of the inter-donor distances in units of a_B are: $l/a_B = 10$ (1), 16.53 (2), 18.6 (3), 23.6 (4), 25.0 (5).

Moreover, for the cases of one and two initial excitations the disentanglement rate is proportional to the decoherence rate of the two-qubit state. In both cases the concurrence attains a stationary and non-vanishing value at large times, which means that phonon scattering does not completely destroy the entanglement of the initially prepared two-qubit state.

The choice of the geometry of the donor sites determines the features of the concurrence as a time-dependent function. These features can be understood by a simple kinetic interpretation of phonon travels among the donor sites. In this work we focused on the cases of initially one and two excitations. However, we believe that also particular superpositions of both cases may be treated within this framework. Furthermore, our model includes already the case of $N > 2$ qubits, where a trace over $N - 2$ qubits would be required to obtain the entanglement between a selected pair of qubits. This will be subject of future work.

Acknowledgments

SW and FL acknowledge support by FONDECYT project no. 1095214. FL acknowledges support from Financiamiento Basal project no. 0807.

-
- [1] M.A. Nielsen and I.L. Chuang, *Quantum Computation and Quantum Information* (Cambridge University Press, Cambridge, 2000)
- [2] C.H. Bennett, G. Brassard, C. Crépeau, R. Jozsa, A. Peres, and W.K. Wootters, Phys. Rev. Lett. **70**, 1895 (1993).
- [3] C.H. Bennett and S.J. Wiesner, Phys. Rev. Lett. **69**, 2881 (1992).
- [4] A.K. Ekert, Phys. Rev. Lett. **67**, 661 (1991).
- [5] D. Leibfried, R. Blatt, C. Monroe, and D. Wineland, Rev. Mod. Phys. **75**, 281 (2003).
- [6] L.M.K. Vandersypen and I.L. Chuang, Rev. Mod. Phys. **76**, 1037 (2004).
- [7] J.M. Raimond, M. Brune, and S. Haroche, Rev. Mod. Phys. **73**, 565 (2001).
- [8] R. Hanson, L.P. Kouwenhoven, J.R. Petta, S. Tarucha, and L.M.K. Vandersypen, e-print cond-mat/0610433.
- [9] B.E. Kane, Nature **393**, 133 (1998).
- [10] L. Dicarlo, J.M. Chow, J.M. Gambetta, L.S. Bishop, B.R. Johnson, D.I. Schuster, J. Majer, A. Blais, L. Frunzio, S.M. Girvin, and R.J. Schoelkopf Nature **460**, 240 (2009).
- [11] T. Gaebel, M. Domhan, I. Popa, C. Wittmann, P. Neumann, F. Jelezko, J.R. Rabreau, N. Stavrias, A.D. Greentree, S. Praver, J. Meijer, J. Twamley, P.R. Hemmer, and J. Wrachtrup, Nature Physics **2**, 408 (2006).
- [12] N.V. Prokof'ev and P.C.E. Stamp, Rep. Prog. Phys. **63**, 669 (2000).
- [13] L. Amico, R. Fazio, A. Osterloh, and V. Vedral, Rev. Mod. Phys. **80**, 517 (2008).
- [14] L. Chirolli and G. Burkard, Adv. in Physics **57**, 225 (2008).
- [15] L.C.L. Hollenberg, A.S. Dzurak, C. Wellard, A.R. Hamilton, D.J. Reilly, G.J. Milburn, and R.G. Clark, Phys. Rev. B **69**, 113301 (2004).
- [16] B. Koiller, X. Hu, and S. Das Sarma, Phys. Rev. B **73**, 045319 (2006).
- [17] A.V. Tsukanov and K.A. Valiev, Russian Microelectronics **36** (2), 6780 (2007).
- [18] D. Stepanenko and G. Burkard, Phys. Rev. B **75**, 085324 (2007).
- [19] H. Zhao and J.B. Freund, J. Appl. Phys. **104**, 033514 (2008).
- [20] F. Lastra, S.A. Reyes, and S. Wallentowitz, J. Phys. B **44**, 015504 (2010).
- [21] F. Lastra, S.A. Reyes, and S. Wallentowitz, Rev. Mex. Fís. **57**, 148 (2011).
- [22] J. Eckel, S. Weiss, and M. Thorwart, Eur. Phys. J. B **53**, 91 (2006).
- [23] A.J. Leggett, S. Chakravarty, A.T. Dorsey, M.P.A. Fisher, A. Garg, and W. Zwerger, Rev. Mod. Phys. **59**, 1 (1987).
- [24] M. Abanto, L. Davidovich, B. Koiller and R.L. de Matos Filho, Phys. Rev. B **81**, 085325 (2010).
- [25] W.K. Wootters, Phys. Rev. Lett. **80**, 2245 (1998).